



# Numerical Simulation of Pitching Sloshing under Microgravity

W. J. Yang<sup>1</sup>, T. T. Zhang<sup>1</sup>, C. Li<sup>1</sup>, S. M. Li<sup>1</sup> and X. H. Xu<sup>2†</sup>

<sup>1</sup> *State Key Laboratory of High Performance Computing, College of Computer, National University of Defense Technology, Changsha 410073, China*

<sup>2</sup> *National Innovation Institute of Defense Technology (NIIDT), Beijing 100060, China*

† *Corresponding Author Email: xuxinhai@nudt.edu.cn*

(Received September 29, 2018; accepted January 12, 2019)

## ABSTRACT

In this paper, the fluid characteristics of pitching sloshing under microgravity condition are investigated. A numerical method by solving the Navier-Stokes equations to study three-dimensional (3-D) nonlinear liquid sloshing is developed with OpenFOAM, a Computational Fluid Dynamics (CFD) tool. The computational method is validated against existing experimental data in rectangular tank under ordinary gravitational field. However under low gravity conditions, the sloshing liquid shows seemingly chaotic behavior and a considerable volume of liquid attaches on the sidewall due to the effect of surface tension, which is verified in simulation experiment. Besides, the nonlinear liquid behaviors in hemi-spherically bottom tank are firstly studied in this paper. It is found that the wave evolution becomes divergent with the decrease of gravitational acceleration. The natural frequency reaches a constant magnitude quickly with the increase of liquid height and then increases again until the filling level exceeds 70%. Meanwhile, the liquid dynamics of forced pitching sloshing under resonant and off-resonant condition are demonstrated respectively. The numerical techniques for 3-D simulation are hopeful to provide valuable guidance for efficient liquid management in space.

**Keywords:** Liquid sloshing; Microgravity; Three-dimensional simulation; Pitching; VOF method.

## NOMENCLATURE

$A$	maximum pitching amplitude	$\vec{x}$	coordinate vector
$Bo$	Bond number	$\mu_{eff}$	effective viscosity
$b$	width of the tank	$\mu$	dynamic laminar viscosity
$F_1$	acceleration due to gravity force	$\nu_t$	turbulence viscosity
$F_2$	acceleration due to surface tension force	$\alpha$	function of volume fraction
$g_0$	acceleration of gravity in ordinary gravitational field	$\theta$	contact angle
$g$	acceleration of gravity	$\rho$	fluid density
$h_0$	height of liquid	$\rho_1$	densities of gas
$\vec{n}$	unitary normal vector	$\rho_2$	densities of liquid
$p$	pressure	$f$	frequency respectively
$r$	radius of tank	$\sigma$	surface tension
$\vec{U}$	velocity vector of the fluid	$f_0$	experimental natural frequency for the liquid height
$V$	volume		
$\nu$	kinematic viscosity		

## 1. INTRODUCTION

The importance of liquid sloshing has been highly recognised with the increasing amount of liquid on board spacecraft and satellites. Liquid sloshing in

tank usually results from the processes of spacecraft orbital transferring, rendezvous and docking. The influence of sloshing fluid probably hamper the liquid storage device and manoeuvres in space. Even the non-linear behaviors of a small amount of fuel

may lead to disastrous consequences (Strikwerda, Ray, Haley, and O'Shaughnessy, 2001). Thus a deep understanding of surface behaviors and stability for different excitations are critical for the design and management of spacecrafts.

Liquid dynamics under microgravity face different problems from those under regular gravitational field (Abramson 1961). Under microgravity conditions, the gravity diminishes and surface tension of the liquid becomes dominant. The liquid volume won't be locate toward the bottom of tank but may be distributed around the tank unpredictably. The study of the liquid dynamics under microgravity has been carried out with theoretical and experimental ways (Ibrahim, Pilipchuk, and Ikeda, 2001; Abramson 1966; Petrash, Zappa, and Otto, 1962; Hastings and Rutherford III, 1968).

Satterlee and Reynolds (Satterlee and Reynolds 1964) successfully solved the free vibration problem for a circular cylindrical tank in low-gravity condition. Yeh (Yeh, 1967) extended the same analysis for axisymmetric tanks. Salzman and Masica (Salzman and Masica, 1967) conducted drop tower experiments to present the liquid reorientation shapes under different Bond numbers (ratio of acceleration to capillary forces) and liquid volumes. For forced sloshing, Dodge and Garza (Dodge and Garza 1967) developed an equivalent mechanical model and simulated experiments to describe sloshing characteristics for cylindrical tanks under lateral motion, including sloshing forces, natural frequencies and slosh damping. In addition, the same works for spherical and ellipsoidal tanks are performed in literature (Dodge and Garza, 1970; Dodge and Garza, 1969). Salzman *et al.* (Salzman and Masica 1969; Coney and Salzman, 1971), using 5-second zero-gravity free-fall facility, conducted experimental investigation to determine the natural frequencies and damping characteristics of lateral sloshing for cylinders and oblate spheroidal tanks. A finite difference technique is developed to solve the lateral sloshing problem in a cylindrical tank with a hemispherical bottom (Concus, Crane, and Satterlee, 1968).

Previous forced liquid sloshing investigations were mostly limited to translation oscillations (Yeh, 1967; Chu, 1970). The pitching excitation combining swaying and rolling should be taken into consideration for analysis of liquid sloshing. Chu (Chu, 1970) developed a semi-numerical approach to estimate forces and moments for an arbitrary axisymmetric tank subjected to pitching oscillation. However the free surface shapes were not considered and sloshing analysis must be modified to account for distortion of free surface in different gravitational field. For the hemi-spherically bottom tank, which has been employed on Sloshsat FLEVO (Vreeburg, 2005) to study solid-liquid interaction dynamics, several relative numerical simulations were given in literature (Veldman, Gerrits, Luppens, Helder, and Vreeburg, 2007; Luppens, Helder, and Veldman, 2009). However the liquid dynamics in tank under pitching excitation have not been studied before. The liquid behavior in microgravity is of great interest for spacecrafts containing liquid tanks and the

magnitude of the liquid natural frequencies and its behavior under forced excitation is of considerable importance for the liquid stability investigations.

To address these issues, the present work conducts a 3-D simulation study on pitching sloshing under low-gravity field. The objectives mainly are as follows: (1) introducing a numerical method with OpenFOAM, which solves the Navier-Stokes equations with finite volume method. (2) verifying the numerical method against existing experimental data in rectangular tank (Armenio and La Rocca, 1996) and revealing the typical sloshing dynamics under microgravity, (3) presenting wave evolutions under different gravitational fields and predicting natural frequencies at different filling levels for hemi-spherically bottom tank, (4) demonstrating the sloshing liquid behaviors in resonant and off-resonant conditions respectively.

In the next section the numerical techniques descriptions are presented, including the governing equations, the discrete method and the volume-of-fluid method, followed by computations of sloshing characteristics. Then the numerical method is applied to liquid sloshing in rectangular tank and is validated by comparing simulation results with experimental data. Moreover, the liquid sloshing dynamics under low-g condition are discussed. Last, as well as the unstructured mesh generation and mesh convergency analysis, predictions for free sloshing and forced pitching sloshing in hemi-spherically bottom tank are demonstrated as a reference for tank design and spacecraft management.

## 2. NUMERICAL TECHNIQUES FOR 3-D SIMULATION

Numerical simulation method is an effective way to handle unsteady nonlinear flows, which generally occur in most cases of liquid sloshing under microgravity. Computational fluid dynamics (CFD) has received highly attention as a powerful tool for the analysis of multiphase flow problems. OpenFOAM is an open source CFD toolbox (Jasak, 2009) and is widely used to simulate multiphase flows (Guo, Yang, Xu, Cao, and Yang, 2015; Zhang, Yang, Lin, Cao, Wang, Wang, and Wei, 2016). In this work, the computations were carried out using OpenFOAM. The numerical method and model problems are introduced in this section. The descriptions of used symbols are given in nomenclature.

### 2.1 The Governing Equations

The presented simulation approach of liquid sloshing under microgravity is solving the Navier-Stokes equations with the finite volume discretization schemes. For an incompressible fluid with constant viscosity, conservation of mass is given by the continuity equation

$$\nabla \vec{U} = 0 \quad (1)$$

and conservation of momentum in three directions is given by

**Table 1 Summary of discretisation schemes**

Term	Form	Scheme	order of accuracy
Gradient term	$grad(\vec{U})$	Gauss linear	second order
Diffusion term	$laplacian(\mu_{eff}, \vec{U})$	Gauss linear corrected	second order
Convective term	$div(\rho\vec{U}\vec{U})$	Gauss limitedLinearV 1 or Gauss vanLeer	first order
Temporal term	$ddt(\rho, \vec{U})$	backward	second order

$$\frac{\partial \rho \vec{U}}{\partial t} + \nabla \cdot (\rho \vec{U} \vec{U}) - \nabla \cdot (\mu_{eff} \nabla \vec{U}) - \nabla \vec{U} \cdot \nabla \mu_{eff} = -\nabla p + F_1 + F_2 \quad (2)$$

In these equations,  $\vec{U}$  is the velocity vector of the fluid,  $p$  denotes the pressure and  $\rho$  denotes the fluid density.  $\mu_{eff}$  is the effective viscosity, which writes

$$\mu_{eff} = \mu + \rho \nu_t \quad (3)$$

where  $\mu$  is the dynamic laminar viscosity and  $\nu_t$  is the turbulence viscosity.

The vectors  $F_1$  and  $F_2$  demonstrate accelerations due to gravity and surface tension force respectively. However, the gravity is nearly neglected while the surface tension force becomes predominant in low-gravity situations. The acceleration of gravity  $g = 10^{-1} g_0 \sim 10^{-6} g_0$ , where  $g_0$  is the acceleration of gravity in ordinary gravitational field.  $F_1$  should be written as

$$F_1 = -g\vec{x}\nabla\rho \quad (4)$$

where  $\vec{x}$  is the coordinate vector. Equations 1 and 2 are relative to frame of reference which is fixed to the moving wall. The boundary conditions of the tank wall and the liquid surface are also considered.

The no-slip condition ( $\vec{U} = 0$ ) is applied at the tank wall, demonstrating that the wall boundary is impermeable and that the liquid sticks to the wall resulting from viscous effects.

Under microgravity, the surface tension cannot be neglected. The free liquid surface is not flat in the tank but rises around the tank wall. The mean curvature of free surface needs to be considered for the calculation of surface tension force, therefore

$$F_2 = \sigma\kappa\nabla\alpha \quad (5)$$

where  $\alpha$  denotes the function of volume fraction and the detailed discussion is given in the description of VOF method. The mean curvature of liquid surface is given by

$$\kappa = \nabla \cdot \left( \frac{\nabla\alpha}{|\nabla\alpha|} \right) \quad (6)$$

The Bond number plays a major role in the free surface characteristics. The calculation of Bond number  $Bo$  is given as

$$Bo = \frac{gr^2}{\sigma/\rho} \quad (7)$$

where  $r$  is radius of tank. Very low-gravity fluid mechanics are characterized by  $Bo < 1$  while high-gravity problems occur for  $Bo > 1000$  (Dodge and Garza, 1967). The Bond number used in the micro-gravity is in the range of 10 to 100.

The contact angle (angle between the normal at the wall boundary and the normal at the free surface) is determined by the properties of liquid, air and tank wall. In this study, the contact angle is assumed to be static and is taken as  $\theta=0$ .

The governing equations 1 and 2 are discretised using finite volume method. Lots of discretisation schemes with different accuracy are provided by OpenFOAM toolbox. Those terms applied for calculation of the governing equations are listed in Table 1.

## 2.2 Surface tracking: VOF method

The volume-of-fluid method is employed to track the free surface of the sloshing liquid. In the VOF method, the immiscible phases are prescribed. The movement of the interface surface is determined by function of volume fraction  $\alpha$ , namely the volumetric ratio of the liquid in a computational cell. In each cell, the volume fraction of all phases sum to unity. The interface surface is obtained through the following three conditions.

$$\alpha(x, y, z, t) = \begin{cases} 1 & \text{liquid} \\ 0 & \text{gas} \\ 0 < \alpha < 1 & \text{mixture} \end{cases} \quad (8)$$

The function of volume fraction  $\alpha$  equals to 0 in air and 1 in liquid, while the value in the mixture cell is in the range of 0 to 1. The continuity equation for the volume fraction of phases has the following form:

$$\frac{\partial \alpha}{\partial t} + \nabla \cdot (\alpha \vec{U}) = 0 \quad (9)$$

The momentum equation 2 is controlled through determining the components of the phases in each cell volume. The average value of density is given as

$$\rho = \alpha.\rho_1 + (1 - \alpha)\rho_2 \quad (10)$$

$\rho_1$  and  $\rho_2$  denote densities of gas and liquid respectively. Other properties are also calculated as the same formula. Thus the value of volume fraction  $\alpha$  at each cell is defined by substituting the average values of properties in the Navier-Stokes and volume fraction equations and the free shape is constructed by applying the free surface reconstruction algorithm during every time step.

### 2.3 Model Problem for Pitching Sloshing

Considering an axisymmetric tank is partially filled with a mass of liquid as shown in Fig. 1. The air fills the remaining part of the closed tank. The characteristic radius of the tank is  $r$  and initially the height of liquid is  $h_0$ . The  $xoy$  coordinate system fixed to the tank is centered at the tank center. The  $XOY$  frame is regarded as space-fixed coordinate system.

The tank, while undergoing a constant vertical gravitational acceleration  $g$ , is imposed by pitching motion with respect to the  $z$ -axis. The interface surface waves under forced oscillation and is described as the function  $h(x,y,z,t)$ , where  $t$  denotes time. Under low-gravity situations, capillary forces predominate and the free surface will not be flat, but rises around the tank wall as the curved dotted line in Fig. 1. When the tank starts pitching, the surface loses stability and oscillates in an seemingly chaotic way. The tank has been forced in pitching motion around the  $z$ -axis. The pitching angle changes as

$$\varphi = A \sin(2\pi ft) \tag{11}$$

Thus the pitching angular velocity is

$$\varepsilon = 2\pi f A \cos(2\pi ft) \tag{12}$$

where  $A$  and  $f$  denote the maximum pitching amplitude and frequency respectively.

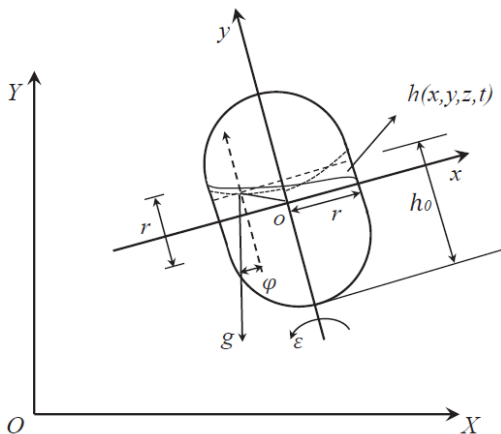


**Fig. 1. Geometry model for pitching oscillation and coordinate system.**

The sloshing characteristics are effective descriptions for the liquid behaviors in oscillating tank, like natural frequencies, forces, and shapes of the free liquid surface. Generally the natural frequency of liquid is the first mode natural frequency. For the computation of natural frequency, some relationships and formulas have been revealed for a certain shape of tank in theoretical and experimental ways (Bauer, 1982; Salzman and Masica, 1967; Salzman, Labus, and Masica 1967). In simulation method, the natural frequency can be estimated in the process of free sloshing after oscillating. Additionally, the sloshing normal force

exerted on the tank by the liquid can be evaluated by integrating the pressure,

$$F = \int_{S_w} p \vec{n} dS \tag{13}$$

where  $\vec{n}$  is the unitary normal vector over the wetted wall surface  $S_w$ , i.e.  $\vec{n} = (n_x, n_y, n_z)$ . The three components of  $F$  along  $x$ ,  $y$  and  $z$  direction respectively are

$$\begin{aligned} F_x &= \int_{S_w} p n_x dS \\ F_y &= \int_{S_w} p n_y dS \\ F_z &= \int_{S_w} p n_z dS \end{aligned} \tag{14}$$

The shapes of free surface and wave heights are extracted by VOF method. The sloshing liquid characteristics in tanks under pitching excitation are studied comprehensively with above methods in this work.

### 3. VALIDATIONS AND DISCUSSION

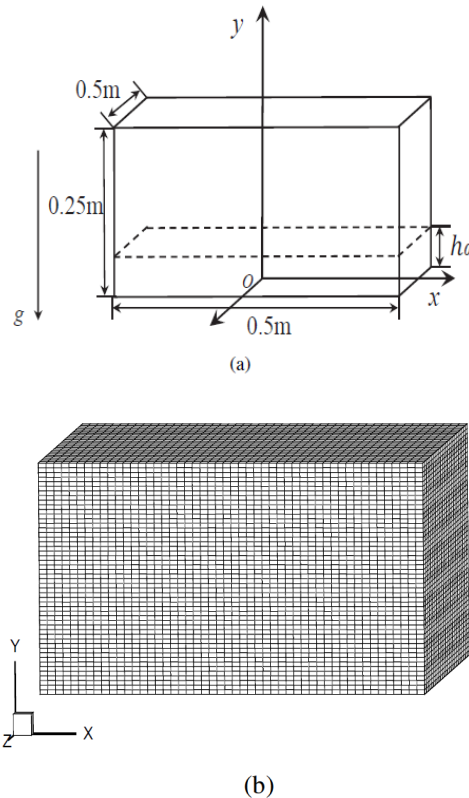
There are two main problems to be handled in present study, one for validations and the other for predictions. For the validations, existing experiments are selected to verify the numerical techniques and the pitching mechanism. In addition, the typical sloshing behaviors under microgravity are reproduced and discussed in the simulation case. The other is prediction of sloshing dynamics in oscillating hemi-spherically bottom tank with the validated 3-D simulation methods, including the time evolutions of wave heights, natural frequencies and forces. In both problems, fresh water (kinematic viscosity  $\nu = 1 \times 10^{-6} m^2 / s^{-1}$ , density  $\rho = 998.2 kg / m^{-3}$ , surface tension  $\sigma = 72.72 \times 10^{-3} kg / s^{-2}$ ) and air at 20°C are chosen as the liquid and gas respectively in the tank.

#### 3.1 Model Validation for Pitching Motion

Since the liquid sloshing dynamics under microgravity are complex and the facilities for microgravity are limited, relative researches on the sloshing liquid dynamics with pitching excitation under microgravity are quite rare, especially the experimental research. For validation purpose, experiment of pitching sloshing in a rectangular tank under ordinary gravitational field (Armenio and La Rocca, 1996) is selected, which is one of the well known experiments for unsteady free surface flows.

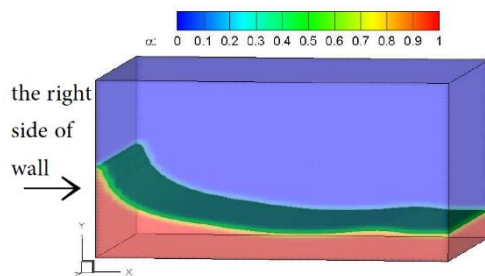
The tank shape is taken from Armenio *et al.* (Armenio and La Rocca, 1996). The dimensions of the tank are 0.5m long, 0.5m wide and 0.25m tall. The tank is filled with water and the liquid height  $h_0 = 0.05m$ . The coordinate system is centered at the bottom center of the tank as shown in Fig. 2(a) and a typical structured mesh for the tank in 3-D simulation is shown in Fig. 2(b). The tank is oscillated by a sinusoidal pitching motion with

respect to the  $z$  axis as described in the above part of the model problem. The maximum excitation amplitude  $A = 0.016$  and the experimental natural frequency for the liquid height  $f_0 = 0.8\text{Hz}$ .



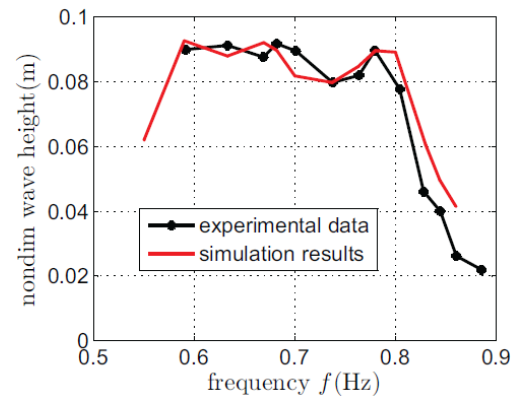
**Fig. 2. (a) Geometry model of rectangular tank and (b) the structured mesh  $50 \times 50 \times 25$  (62500 cells).**

Fig. 3 shows the 3-D free surface shape at  $t = 4.5\text{s}$  under forced pitching oscillation ( $A = 0.016$ ,  $f = 0.8\text{Hz}$ ). The snap shot is selected for comparison with experimental data. The function of volume fraction  $\alpha$  is set to determine the interface surface in VOF method. The red area represents water ( $\alpha = 1$ ) while the blue is air ( $\alpha = 0$ ). The interface surface is colored by green ( $0 < \alpha < 1$ ). It is shown that the surface waves and reaches the highest sloshing amplitude at the side of the tank. The impacting on the vertical tank walls appears even though the amplitude of excitation is small. The surface shape is nearly the same as that obtained in experiments.



**Fig. 3. The 3-D free surface shape under pitching sloshing at  $t = 4.5\text{s}$ .**

Numerical simulations are continued with a wide range of excitation frequencies, from  $f = 0.4\text{Hz}$  to  $f = 1.1\text{Hz}$ . In Fig. 4 the measured and simulated non dimensional wave heights  $(h_{max} / h_{min}) / b$  versus oscillation frequency are plotted, where  $b$  is the width of the tank and equals to  $0.5\text{m}$ . The non dimensional wave heights are recorded at the location  $x = 0.15\text{m}$  in the experiment. It can be observed that when the oscillation frequency is small the wave height is enlarged with the increasing frequency. While the hydraulic decrease appears when the frequency exceeds the value around  $0.8\text{Hz}$ . The same trend is also observed in simulated results which agree well with the experimental data. In the experiments the resonance phenomenon is observed when the jump appears. The experimental resonance frequency is  $0.804\text{Hz}$  and that predicted by the 3-D simulation method is  $0.78\text{Hz}$ . The relative difference is less than 3%. Armenio (Armenio and La Rocca, 1996) also pointed out that it was difficult to read the experimental signal exactly due to some irregular 3-D wave patterns especially for resonance conditions. So the difference between numerical and experimental results is accepted even the comparison is not completely perfect. It is concluded that the 3-D numerical method and the pitching mechanism applied in present study are effective to study the pitching sloshing.



**Fig. 4. Simulated and experimental non dimensional wave height at location  $x = 0.15\text{m}$  versus oscillation frequency ( $A = 0.016$ ).**

### 3.2 Oscillating Rectangular Tank under Low- Gravity Field

The value of gravitational acceleration has great effect on the liquid behaviors in sloshing tank. In order to evaluate the influence of gravitational acceleration on the liquid sloshing, two simulation cases under ordinary gravity field  $g = g_0$  and micro-gravity field  $g = 10^{-3}g_0$  respectively are computed with the 3-D simulation techniques. The relation between gravity and surface tension is also represented by Bond number  $B_o$ .

In Fig.5 the time-histories of the computed wave height at the right wall under ordinary gravity field and low-gravity field are plotted respectively for  $f =$

0.78Hz (resonance condition). In high-g field ( $g = g_0$ ) the solution shows the overlapping of short waves and large impacting over the wall of the tank. Meanwhile the asymmetric wave shape (the peaks are largely greater than the troughs) is obviously observed, indicating that the liquid sloshing under pitching oscillating contains non-linear and complicated phenomena compared to other forced sloshing. The simulation resolution is in a good agreement with the experimental result (Armenio and La Rocca, 1996).

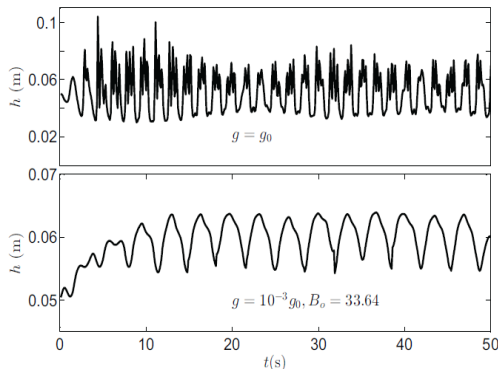


**Fig. 5. Computed time evolution of the wave height at the right side of wall  $x = 0.25$  ( $A = 0.016$ ,  $f = 0.78\text{Hz}$ ,  $h_0 = 0.05\text{m}$ ).**

Instead, The liquid behavior under low-gravity field for the same tank and same liquid volume is quite different. In the microgravity field with acceleration of gravity  $g = 10^{-3}g_0$  and Bond number  $B_o = 33.64$ , it is observed that the surface height initially rises under pitching oscillation and then achieves fluctuating stably. At the initial period the interface surface migrates upward along the wall and the amount of liquid taking part in low-gravity sloshing is less than that for high-g sloshing. The amplitude of fluctuating is also smaller than that of high-g sloshing. Under low-g field, the liquid surface gets a higher fluctuating position and will not recover to the initial liquid position  $h_0$ . The numerical results above agree well with the conclusions of Dodge (Dodge and Garza, 1967) and Bauer et al. (Bauer and Eidel 1989).

#### 4. Results Of 3-D Liquid Sloshing In Hemi-Spherically Bottom Tank

Based on the analysis of the 3-D simulation results for pitching sloshing in rectangular tank, the 3-D simulation method for pitching sloshing has been validated. It is also observed that the non linear features of liquid sloshing appear under pitching oscillation. Moreover the liquid sloshing under micro-gravity becomes seemingly chaotic and the reorientation of the liquid in the tank is more difficult to handle than that in ordinary gravitational field. Therefore the liquid behaviors under forced pitching excitation in microgravity are of considerable

importance for the satellites investigations.

In this section, the liquid motion in hemi-spherically bottom tank is considered. We shall predict the liquid behavior in both free liquid sloshing and pitching forced sloshing cases with the verified 3-D numerical techniques. The influence of gravitational acceleration on liquid sloshing height and the dependence of between the natural frequency on the liquid depth are also analysed. This work will serve a basis for presenting the sloshing features under forced pitching excitation for the shape of tank.

The cylindrical shaped tank with hemispherical ends (as shown in Fig. 1. with a volume of  $V = 86.9L$ , is contained in satellite Sloshsat FLE-VO (Vreeburg, 2005). The tank radius is  $0.228\text{m}$  and the length of cylindrical part (the rest part of the tank except the two hemispherical ends) is equal to radius. The water mass is  $M = 33.5\text{kg}$  and the initial depth  $h_0 = 0.267\text{m}$ . For the hemi-spherically bottom tank cases, the 3-D unstructured grid M2 is generated as shown in Fig. 6(a), consists of 44499 cells with the cell interval size being  $0.025\text{m}$ . Fig. 6(b) shows a 3-D free surface shape at time  $t = 1\text{s}$  in a simulation case where the tank is forced to translate in the lateral direction with a velocity  $v = 0.1\text{m/s}$ . It is observed that large amount of liquid impacting on the sidewall due to the translation. The surface is still continuous because the excitation velocity is small.

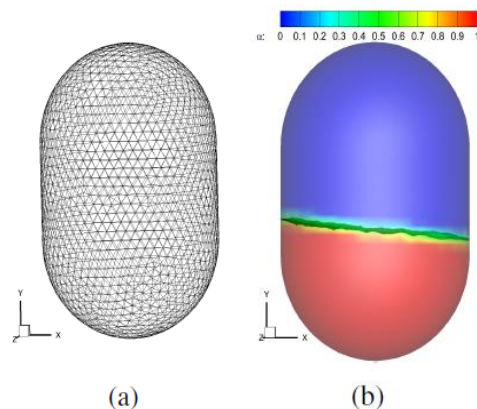


**Fig. 6. (a) Unstructured grid M2 for hemi-spherically bottom tank case. (b) A 3-D free surface shape at a certain instant under lateral linear excitation.**

In order to evaluate the grid dependence of the solutions, the coarse and fine unstructured grids are also generated by halving and doubling the interval size resulting in M1 (5984 cells) and M3 (307847 cells), respectively. The grid convergency analysis is performed by comparing the difference between surface shapes obtained with the three meshes. As shown in Fig. 7, the surface shapes obtained with M2 and M3 are almost identical and the maximum relative difference is less than 2%. So a converged simulation result is achieved with M2, which is adopted in the following simulations for the computing efficiency.

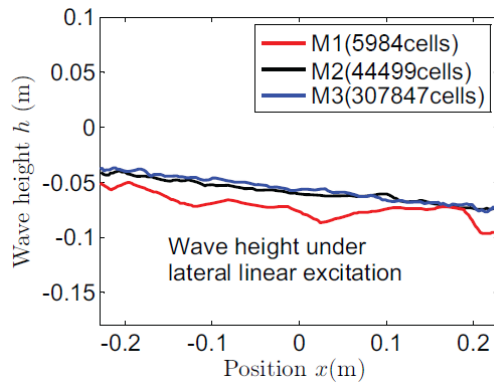


**Fig. 7. Convergence analysis for hemispherically bottom tank.**

#### 4.1 Free Sloshing

The 3-D liquid free sloshing in the hemispherically bottom tank will be studied in the following paragraphs. In 3-D simulation cases, sloshing is induced by oscillating the tank at 2Hz frequency with 0.01m amplitude with respect to the z axis. In order for the liquid to reach maximum amplitude at 2Hz, the tank is excited for 3 seconds. After 3 seconds, the sloshing liquid is allowed to damp naturally.

Time evolutions of the components of normal force on wall under ordinary gravitational field are displayed in Fig.8. Under the pitching oscillating with respect to the z axis, the x component of normal force  $F_x$  is in a harmonic evolution with the frequency at 2Hz in the time period of 0 – 3s. Once the excitation is stopped, the amplitude of  $F_x$  decreases with the increase of time due to the stabilizing effect of gravity. Instead, the components  $F_y$  and  $F_z$  fluctuate slightly around the value of 0. It is worth mentioning that in the excitation period the peaks of  $F_x$  are largely greater than the troughs and the force magnitude never returns to the value of 0 any more in the free sloshing period. These simulation results above illustrate the non-linear and complex features in large-amplitude liquid sloshing under pitching excitation.

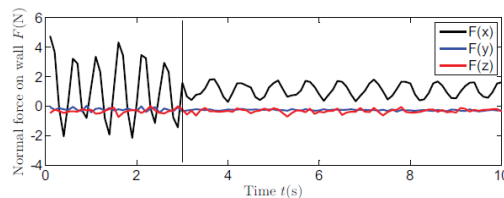


**Fig. 8. Normal force on wall for free sloshing ( $A = 0.01, f = 2\text{Hz}$ ).**

Several simulation cases for free sloshing under different gravitational field with  $g = g_0 \sim 10^{-3} g_0$  are also computed with the 3-D simulation techniques. The comparisons of the time evolutions of wave heights in each case are plotted in Fig. 9. The wave heights are measured at the right side-wall  $x =$

0.228. In the time period 0 – 3s, the tank is excited with the maximum excitation amplitude  $A = 0.01$  and frequency  $f = 2\text{Hz}$ . It is seen from the simulation results that the changes of wave height in each case are obviously different. Under the ordinary gravitational field  $g = g_0$ , the wave still oscillate with decaying amplitude in the period of free sloshing. With the decrease of gravitational acceleration ( $g = 10^{-1} g_0$ ), the liquid rarely fluctuates and the wave amplitude also decreases. In the case with  $g = 10^{-2} g_0$ , the wave height develops differently. In the excitation time 0 – 3s the wave also climbs upward besides oscillating. Once the excitation is stopped, the wave height does not fluctuate but increases and never returns to the initial liquid depth. The same divergency characteristic is also observed under the field  $g = 10^{-3} g_0$  and the wave height is higher than that obtained in the field  $g = 10^{-2} g_0$ .

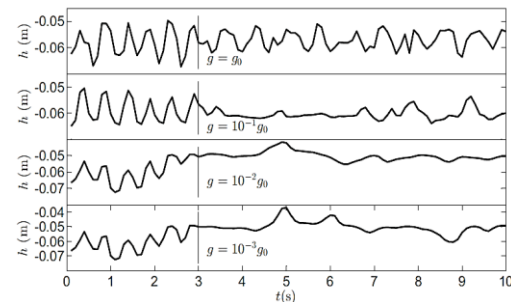


**Fig. 9. Computed time evolution of wave height at the right side of wall  $x = 0.228\text{m}$  for free sloshing under different gravitational field ( $A = 0.01, f = 2\text{Hz}$ ).**

With the decrease of gravitational acceleration, the fluctuating characteristic is not more obvious. Instead the wave height increases and develops as an seemingly chaotic way in the period of free sloshing. Those phenomena under microgravity are resulting from increasing dominant role of surface tension and diminutive stabilizing effect of regular gravitational potential.

#### 4.2 Nonlinear Pitching Forced Sloshing

In the process of free sloshing the sloshing wave attains natural frequency  $f_0$ . For the contact angle  $\theta = \pi / 2$ , the natural frequencies are evaluated and presented in Fig. 10 as a function of liquid height ratio  $h_0 / r$ . The range of frequency in all the simulations are in first mode. In Fig. 10 the natural frequencies at different filling levels ( $V_w / V \in [10\%, 20\%, \dots, 50\%, \dots, 90\%]$ ,  $V_w$  is the volume of liquid) are dotted and the fitting curve is drawn to match them. It may be seen that a constant magnitude is reached quickly, at which no further change occurs with the increase of liquid height until the filling level reaches 70%. When the filling level exceeds 70% the natural frequency starts increasing slightly. It may be imagined that when the filling level is

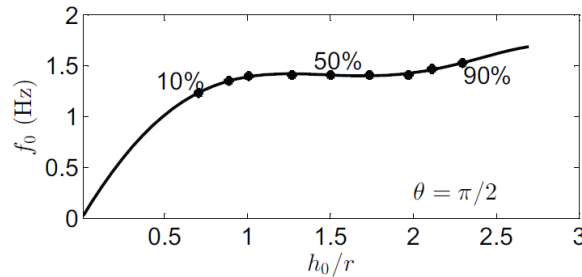


**Fig. 10.** Natural frequencies  $f_0$  of the liquid as a function of the liquid height ratio  $h_0/r$ .

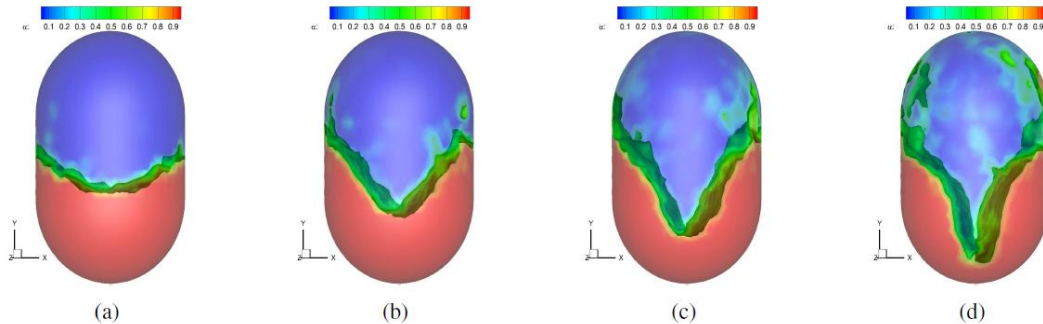


**Fig. 11.** Snap shots of free surface during 3-D forced pitching sloshing at  $t = 10, 20, 30$  and  $40s$  ( $A = 0.01, f = 1.4Hz$ )

100% ( $h_0 / r = 3$ ), namely the tank is full of water, the natural frequency tends to be infinite.

In this part, the demonstrations will be further made by using the present simulation techniques to study forced sloshing in a pitching excited 3-D hemispherically bottom tank with liquid mass of  $M = 33.5kg$ . In these cases the acceleration of gravity is set as  $g = 10^{-3}g_0$  and the Bond number  $B_0 = 70$ .

Since the natural frequencies at different filling levels are determined, the numerical test with the natural frequency is conducted in order to investigate the non-linearity and resonance phenomenon of sloshing under the pitching motion. From the numerical results in Fig. 10, we choose  $f = 1.412Hz$  for filling level of 38.5%. The simulation runs up to  $t = 50s$  and the natural frequency is maintained during entire simulation which ensures that the sloshing liquid reaches maximum amplitude. The maximum excitation amplitude is set as  $A = 0.01$ . The snap shots of the free surface at  $t = 10, 20, 30$  and  $40s$  are shown in Fig. 11, where we can see the obvious 3-D free surface. The relative time evolutions of the  $x$  component of normal force  $F_x$  and wave heights measured on both the right ( $x > 0$ ) and left ( $x < 0$ ) sidewalls are plotted in Fig.12.

Under forced pitching excitation with respect to  $z$  axis, especially with the resonant frequency, the free surface rises quickly around the sidewall and the wave heights also increase continuously at the first time  $t = 10s$ . With the increase of time, the rising amplitude also increases and the development of wave heights on the right and left sidewall become

inconsistent gradually. At the time  $t = 20s$ , the surface starts splashing as a discrete way and beat vibration phenomenon occurs. Then the wave heights become totally divergent and the broken surface climbs nearly on the top of the tank when  $t = 40$ . It can be imagined that the liquid will not exist as a whole but almost migrate to the sidewalls as long as the simulation time is enough long. As well as the liquid mass, the migration time is also relative with the excitation amplitude and frequency. For a constant liquid mass, the wave height reaches the fastest rising velocity and  $F_x$  reaches the maximum magnitude under resonance condition.

Under the same pitching excitation way, demonstrations with off-resonant excitation frequency are also conducted as shown in Fig. 13 and Fig. 14. The maximum excitation amplitude is still  $A = 0.01$  and the frequency is increased to  $f = 2.8Hz$ . Although the excitation frequency is greater than the natural frequency, it is clear that the motion of the sloshing liquid in the tank is much gentle. The crescent shape is not obvious until  $t = 20$ . The rising amplitude also increases with the increase of time. However the liquid slashing and beat vibration phenomenon occurs until  $t = 30$ . It is also seen from Fig. 14 that the wave heights at both sidewalls rise continuously in the entire simulation time and still not reach the maximum amplitude obtained in resonance condition. Likewise, the magnitude of  $F_x$  is much lower than that in resonance condition.

From the simulation results above, it is seen that the forced pitching sloshing under low-g field contains abundant nonlinear phenomena. Under the forced

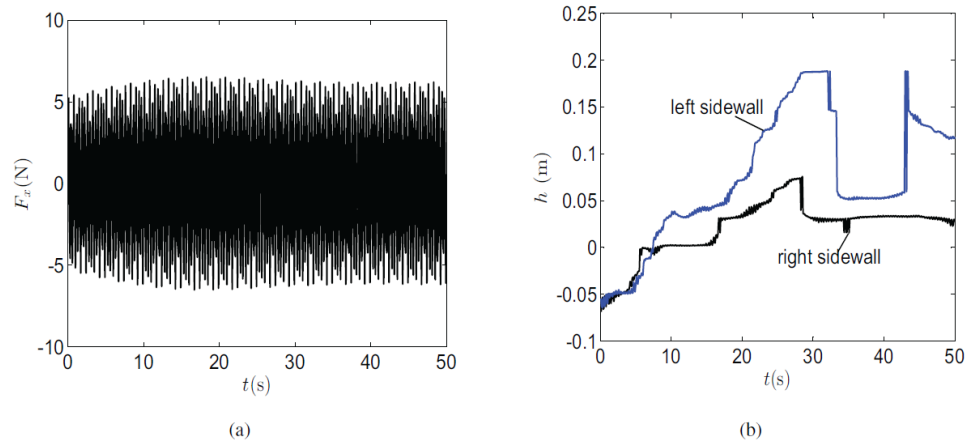


**Fig. 12.** Time evolutions of the x component of normal force  $F_x$  and wave heights during 3-D forced pitching sloshing in resonant condition ( $A = 0.01, f = 1.4\text{Hz}$ ).

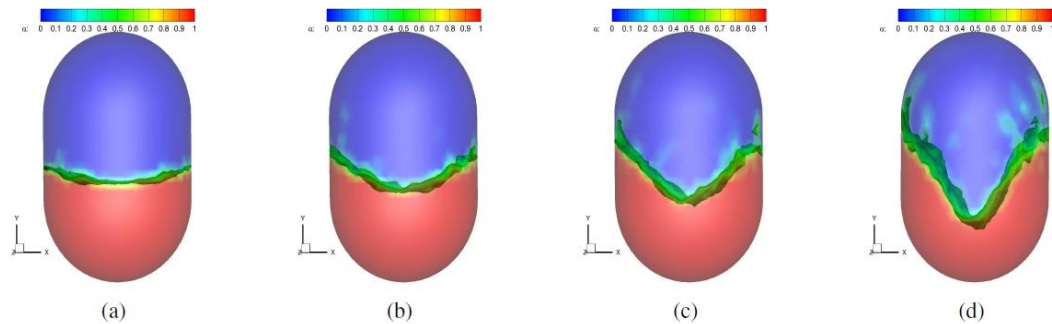


**Fig. 13.** Snap shots of free surface during 3-D forced pitching sloshing at  $t = 10, 20, 30$  and  $40\text{s}$  ( $A = 0.01, f = 2.8\text{Hz}$ ).

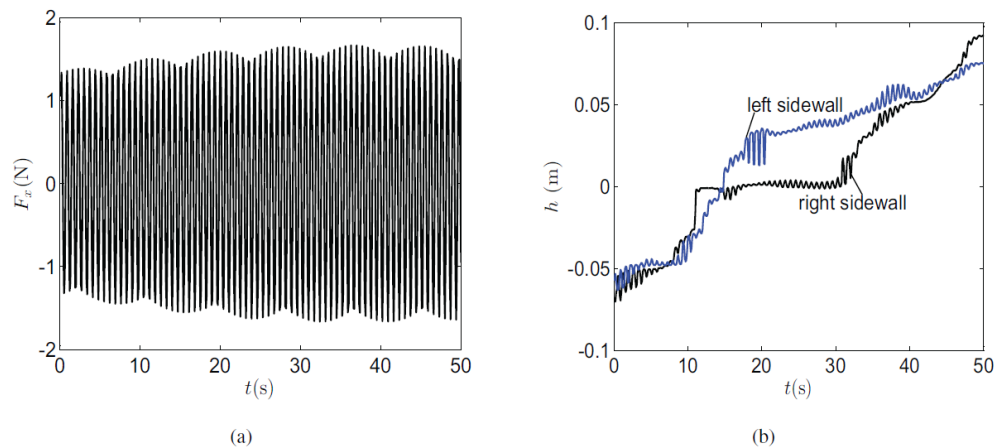


**Fig. 14.** Time evolutions of the x component of normal force  $F_x$  and wave height during 3-D forced pitching sloshing in resonant condition ( $A = 0.01, f = 2.8\text{Hz}$ ).

pitching excitation, the liquid does not wave but rises around the sidewall and can assume any location inside the tank due to the surface tension. The liquid behaviors is relative to the excitation frequency. When the frequency is too small or large away from the natural frequency, the liquid tends to be in lateral periodic motion. Once the frequency is set as the natural frequency, the resonant phenomenon is

observed and the liquid presents swaying and rotating motion. The wave rises quickly up to the top of tank and the broken liquid volume develops divergently. Of course the filling level and excitation amplitude should be taken into consideration in the contribution for the nonlinear features. More simulation experiments are needed for the investigation.

## 5. CONCLUSION

The fluid sloshing under microgravity has been a hot topic and especially the nonlinear sloshing under rotational disturbance like pitching excitation attracts spread attention at present. In this work liquid sloshing under microgravity is studied solving the Navier-Stokes equations. The VOF method is employed to track the free surface of liquid. The governing equations are discretized by second order schemes using the finite volume method.

At first the 3-D simulation approaches and the pitching excitation mechanism are verified with the forced pitching sloshing in rectangular tank under ordinary gravity field, the 3-D results show a good agreement with experimental data. With the same excitation amplitude and frequency, the mass of sloshing liquid under the low-g field reduces and the wave climbs upward the wall, indicating that the increasing effect of surface tension should be taken into account while decreasing the gravitational acceleration.

The both free sloshing and forced sloshing in hemispherically bottom tank under microgravity are studied using the validated numerical techniques. Firstly the grid convergency is accessed and analysed. The nonlinear features of the normal force and wave heights in pitching sloshing are demonstrated, which are more obvious with the decrease of gravitational acceleration. Meanwhile the natural frequencies at different filling levels are evaluated for the contact angle  $\theta = \pi / 2$ .

Furthermore, sloshing liquid behaviors under resonance condition are perfectly reproduced in 3-D simulation. The sloshing characteristics under forced pitching excitation with different excitation frequencies are also studied in detail respectively. The present numerical techniques can be employed to evaluate the general behaviors of liquid sloshing and the results can serve as a basis for the sloshing experiments on spacecraft.

## ACKNOWLEDGMENTS

The authors declare that there is no conflict of interest regarding the publication of this paper. This work was supported by the National Natural Science Foundation of China (No. 61872380) and the National Key Research and Development Program of China (No. 2016YFB0201301).

## REFERENCES

Abramson, H. N. (1961). Liquid dynamic behavior in rocket propellant tanks. *In ONR/AIA Symposium on Structural Dynamics of High Speed Flight* 287–318.

Abramson, H. N. (1966). The dynamic behavior of liquids in moving containers. Nasa sp-106. *Nasa Special Publication* 106(7).

Armenio, V. and M. La Rocca (1996). On the analysis of sloshing of water in rectangular

containers: numerical study and experimental validation. *Ocean Engineering* 23(8), 705–739.

Bauer, H. F. (1982). Coupled oscillations of a solidly rotating liquid bridge. *Acta Astronautica* 9(9), 547–563.

Bauer, H. F. and W. Eidel (1989). Small amplitude liquid oscillations in a rectangular container under zero-gravity. NASA STI/Recon Technical Report N 90, 16167.

Chu, W.H. (1970). Low-gravity fuel sloshing in an arbitrary axisymmetric rigid tank. *Journal of Applied Mechanics* 37(3), 828–837.

Concus, P., G. Crane and H. Satterlee (1968). Low gravity lateral sloshing in a hemispherically bottomed cylindrical tank. Stanford University Press (June 7-18).

Coney, T. A. and J. Salzman (1971). Lateral sloshing in oblate spheroidal tanks under reduced- and normal-gravity conditions. NASA TN-D-6250.

Dodge, F. T. and L. R. Garza (1967). Experimental and theoretical studies of liquid sloshing at simulated low gravity. *Journal of Applied Mechanics* 34(3), 555–562.

Dodge, F. T. and L. R. Garza (1969). Slosh force, natural frequency, and damping of low-gravity sloshing in obliterated ellipsoidal tanks. Report, Technical Report.

Dodge, F. T. and L. R. Garza (1970). Simulated low-gravity sloshing in spherical, ellipsoidal, and cylindrical tanks. *Journal of Spacecraft and Rockets* 7(2), 204–206.

Guo, X. W., W. J. Yang, X. H. Xu, Y. Cao and X. J. Yang (2015). Non-equilibrium steady states of entangled polymer mixtures under shear flow. *Advances in Mechanical Engineering* 7(6), 1–10.

Hastings, L. J. and R. Rutherford III (1968). Low gravity liquid-vapor interface shapes in axisymmetric containers and a computer solution. NASA TM X-53790.

Ibrahim, R. A., V. N. Pilipchuk and T. Ikeda (2001). Recent advances in liquid sloshing dynamics. *Applied Mechanics Reviews* 54(2), 133–199.

Jasak, H. (2009). Openfoam: Open source CFD in research and industry. *International Journal of Naval Architecture and Ocean Engineering* 1(2), 89–94.

Luppés, R., J. A. Helder and A. E. Veldman (2009). The numerical simulation of liquid sloshing in microgravity. *Computational Fluid Dynamics* 2006, 607–612.

Petrash, D. A., R. F. Zappa and E. W. Otto (1962). Experimental study of the effects of weightlessness on the configuration of mercury and alcohol in spherical tanks. Report, DTIC Document.

Salzman, J. A. and W. J. Masica (1967). Experimental investigation of liquid-propellant

- reorientation. National Aeronautics and Space Administration.
- Salzman, J. A. and W. J. Masica (1969). *Lateral sloshing in cylinders under low-gravity conditions*. National Aeronautics and Space Administration.
- Salzman, J. A., T. L. Labus and W. J. Masica (1967). *An experimental investigation of the frequency and viscous damping of liquids during weightlessness*, Volume 4132. National Aeronautics and Space Administration.
- Satterlee, H. and W. Reynolds (1964). The dynamics of the free liquid surface in cylindrical containers under strong capillary and weak gravity conditions. Rep. no. lg-2.
- Strikwerda, T., J. Ray, D. Haley and D. O'Shaughnessy (2001). Near shoemaker-major anomaly survival, delayed rendezvous and mission success. *In Guidance and control 2001*, 597–614.
- Veldman, A. E., J. Gerrits, R. Luppens, J. A. Helder and J. Vreeburg (2007). The numerical simulation of liquid sloshing on board spacecraft. *Journal of Computational Physics* 224(1), 82–99.
- Vreeburg, J. (2005). Measured states of slosh-sat flevo. In 56th International Astronautical Congress. *International Astronautical Federation*, Paper IAF-05-C1.
- Yeh, G. C. (1967). Free and forced oscillations of a liquid in an axisymmetric tank at low-gravity environments. *Journal of Applied Mechanics* 34(1), 23–28.
- Zhang, T. T., W. J. Yang, Y. F. Lin, Y. Cao, M. Wang, Q. Wang and Y.X. Wei (2016). Numerical study on flow rate limitation of open capillary channel flow through a wedge. *Advances in Mechanical Engineering* 8(4), 1687814016645487.